Department of Electrical and Computer Systems Engineering

Technical Report MECSE-18-2005

DWDM ADVANCED OPTICAL COMMUNICATION - Part V: Long and DPSK Simulink Modeling and Experimental Demonstration Test-Beds

Huynh Thanh Liem, Le nguyen Binh and Lam Quoc Huy

MONASH UNIVERSITY

DWDM ADVANCED OPTICAL COMMUNICATION:

Part V: Long-haul ASK and DPSK Simulink Modeling and Experimental Demonstration Test-Beds

Huynh T.L., Binh L.N.,Lam Q.H. and Tran D.D
Department of Electrical and Computer Systems Engineering,
Monash University, Clayton Victoria 3168 AUSTRALIA
e-mail correspondence: le.nguyen.binh@eng.monash.edu.au

***Abstract*—We present the Matlab™ Simulink model and its corroboration with experimental transmission of amplitude and differential phase modulation incorporating RZ, NRZ, carrier suppressed RZ formats over 320 km long-haul optical fibre transmission systems. Dispersion tolerance of the transmission systems under non-compensation and compensated transmission fibres is given. Simulated and measured eye diagrams are reported.**

***Index Terms*—Fibre nonlinear effects, DPSK modulation, standard single mode fibre, DWDM, Simulink.**

TABLE OF CONTENTS

1 INTRODUCTION

In recent years, the capacity and reach distance of optical transmission systems have dramatically increased due to accelerating growth of data usage demand (Internet, Peer-to-Peer network…). Therefore, the necessity of upgrading of current DWDM 10Gbps systems to DWDM 40Gbps or even higher bit rates becomes crucial to telecommunications service providers. Accordingly several modulation formats have been proposed and investigated as the alternatives for the current On-Off Keying (OOK) intensity modulation that is severely degraded at high bit rate due to dispersion and nonlinear effects of the transmission fibers. Apart from the requirements of robustness to the transmission impairments, the cost effectiveness for the system up-grades is also significant. Among the candidates, differential binary/quadrature phase shift keying (DPSK/DQPSK) have recently attracted much attention due to the following advantages: (i) 3-dB improvement on receiver sensitivity (if balanced receiving technique is used) [1, 2]; (ii) high tolerance to fiber nonlinearities, especially to intra-channel nonlinear effects, We present the cross phase modulation (XPM) and the four wave mixing (FWM)[2, 3]; (iii) superior spectral efficiency (DQPSK), hence high tolerance to optical filtering [4] ; and finally, (iv) advantages in all-optical networks incorporating optical add-drop multiplexers or optical cross-connects [5]. Recently, several experimental demonstration of DPSK/DQPSK long–haul transmission DWDM systems for 10Gbps and 40Gbps have been reported [6-8]. Therefore, the need of a simulation testbed is of strong interests for convenience of design, investigation and verification on benefits and shortcomings of advanced modulation formats on the transmission system. In this paper, we present, to the best of our knowledge, the first Matlab^{TM}Simulink-based simulation package for photonic DWDM systems. The simulator is still in the first phase of the development, where the focus is on single-channel system and it is continuously improved and updated. Further we present our ASK and DPSK transmission experimental results conducted in the collaborative transmission test-bed of Monash University, SHF Communications Technology AG - Germany and Telstra Corporation (Research Laboratories). The dispersion tolerances of the system are measured for DPSK and ASK modulation formats with RZ, NRZ and CSRZ.

The paper is structured as follows: (i) in Section II, the fundamentals for the modeling of DPSK transmission system are given; (ii) Section III presents the architecture and operational principles of

the Simulator; (iii) Section IV present simulation results of the up-to-date Simulator and the corroboration of the developed models in comparison with experimental results are presented in Section V for both ASK and DPSK modulation formats. Finally concluding remarks are given.

2 FUNDAMENTALS OF DPSK TRANSMISSION SYSTEMS

The schematic diagram of a single-channel DPSK system is illustrated in Fig. 1 The principal operations of the system can be described in the following.

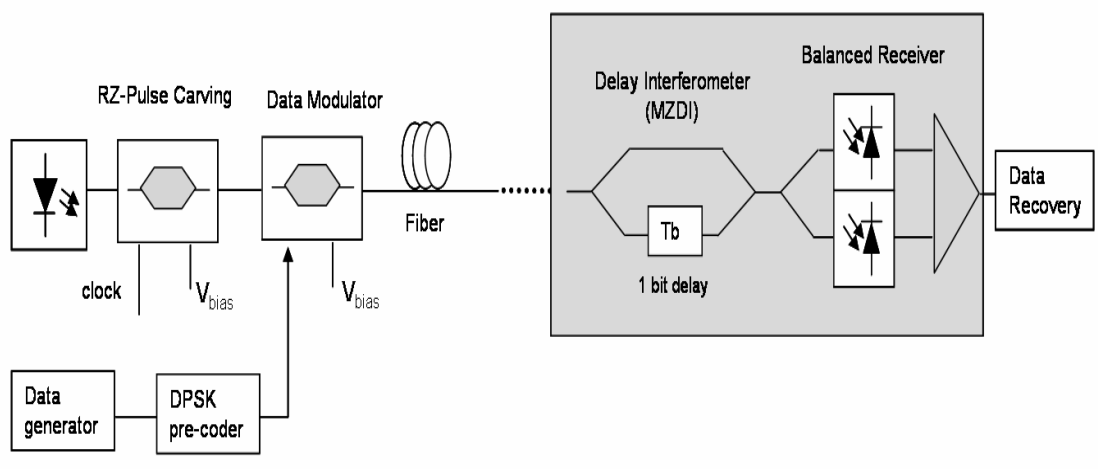

Fig. 1. General block diagram of the single-wavelength channel DPSK optical fibre transmission system.

2.1 DPSK Transmitter

The DPSK transmitter consists of three sections: the optical modulation, the electronic coding and electrical microwave power amplifiers for driving the electrodes of the modulators. The optical modulation sections employs two x-cut single drive $LiNbO_3$ Mach-Zehnder intensity modulators (MZIM): the first MZM generates RZ pulse trains of carrier-modulated lightwaves, hence the RZ format and thus called the “pulse carver”. The second MZM is the data modulator and is driven by the coded sequence from the pre-coder whose structure for DPSK formats is shown in Fig. 2

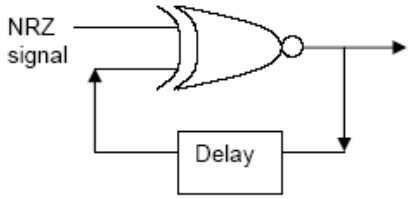

Fig. 2. DPSK pre-coder

The transmitted optical field *E(t)* at the output a MZIM as a function of the driving and bias voltages can be written as

$$E(t) = E_0 \cos\left(\frac{\pi}{2}\frac{V_t + V_b}{V_\pi}\right) \tag{1}$$

where E_o is the transmitted light electric field, V_t is the time-varying signal voltage, V_b is the DC bias voltage applied to the modulator, V is the drive voltage creating π phase shift in the MZM.

2.2 DPSK Balanced Receiver

The delay balanced receiver is shown at the right side in Fig. 1 in which the optical field received is split into two arms, one delayed by a symbol period and no delay. The received signal at the output of the balanced receiver is given as [9]:

$$\begin{aligned} P_D(t) &= \left|E_D(t) + E_D(t-\tau)\right|^2 - \left|E_D(t) - E_D(t-\tau)\right|^2 \\ &= 4\Re\left\{E_D(t)\right\} E_D^*(t-\tau) = \cos\left(\Delta\phi + \varsigma\right) \end{aligned} \tag{2}$$

where $E_D(t)$ and $E_D(t-\tau)$ are the current and the 1-bit delay version of DPSK signals at the delay interferometer. respectively. $\Delta\phi$ and ς represent the differential phase and the phase noise caused by nonlinear phase noise or the MZ delay interferometer imperfections (MZDI). The later issue is not a severe degradation factor due to the high stability of planar lightwave circuit MZDI using a thin-film heater for tuning any waveguide path mismatch.

2.3 RZ pulses in MZM.

Three different types of RZ pulses can be generated, that depends on the voltage biasing schemes of the MZIM. The equations governing the RZ pulses electric field waveforms are [10]

$$E(t)=\begin{cases}\dfrac{1}{\sqrt{E_b}}\sin\left[\dfrac{\pi}{2}\left(1+\sin\left(\dfrac{\pi t}{T_b}\right)\right)\right] & \text{33\% duty-ratio RZ pulses}\\ \dfrac{1}{\sqrt{E_b}}\sin\left[\dfrac{\pi}{4}\left(1+\cos\left(\dfrac{2\pi t}{T_b}\right)\right)\right] & \text{50\% duty-ratio RZ pulses}\\ \dfrac{1}{\sqrt{E_b}}\sin\left[\dfrac{\pi}{2}\cos\left(\dfrac{\pi t}{T_b}\right)\right] & \text{67\% duty-ratio RZ pulses}\end{cases} \tag{3}$$

where E_b is the pulse energy per transmitted bit.

The first type 33% duty-ratio RZ pulses are commonly known as "carrier max or conventional" (C-RZ) pulses and has the pulse width of approximately 9-12 ps whereas the 67% duty cycle RZ pulses whose pulse width is approximately 15 ps are normally known as carrier-suppressed (CS-RZ) pulses. The art in generation of these two RZ pulse types stays at the difference of biasing voltage. The bias voltage conditions and the pulse shape of these two RZ types are illustrated in Fig. 3

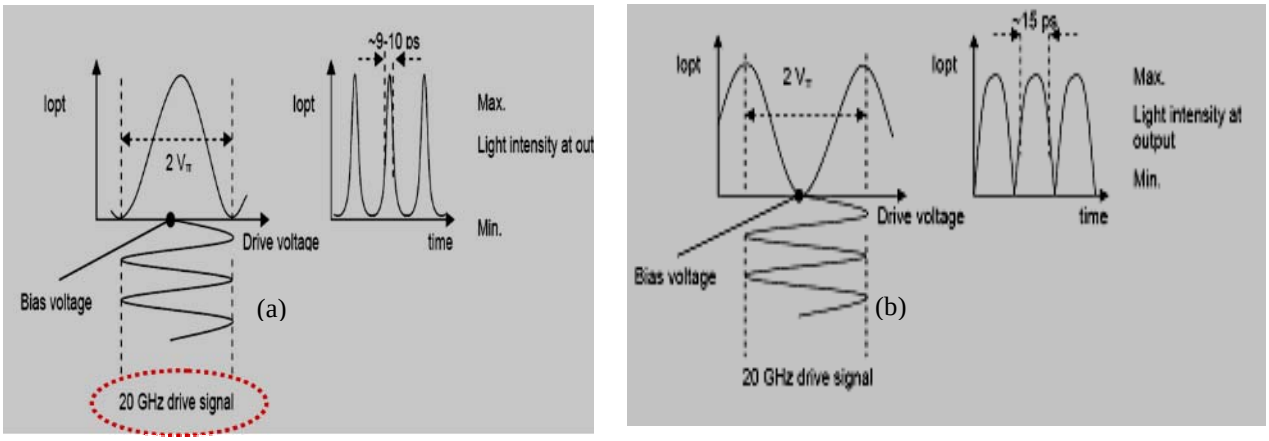

Fig. 3. Electric field waveforms of RZ-optical pulses [11] (a) Carmax RZ pulse; b) CS-RZ pulses

2.4 Fiber Propagations for single channel and transmission impairments

The propagation evolution of the complex envelope A(z,t) of optical electric field signals along a nonlinear optical fiber is governed by the well-known nonlinear Schroedinger equation (NLSE):

$$\frac{\partial A(z,t)}{\partial z}+\frac{\alpha}{2}A(z,t)-\frac{j}{2}\beta_2\frac{\partial^2 A(z,t)}{\partial t^2}-\frac{1}{6}\beta_3\frac{\partial^3 A(z,t)}{\partial t^3}=-j\gamma\left|A(z,t)\right|^2A(z,t) \tag{4}$$

where z is the spatial longitudinal coordinate, α accounts for fiber attenuation, β_2 and β_3 represent fibre dispersion and γ is the nonlinear coefficient. Eq. (4) involves chromatic dispersion, high-order

dispersion, attenuation and SPM of a single-channel transmission fiber. In our developed Simulink-based simulator, the symmetric Split-Step-Fourier method is utilized and optimized.

Currently the Simulator the single channel transmission system is playing a really crucial in evaluation the performance of high capacity and long-haul DWDM transmission system. It has been reported that DPSK/DQPSK DWDM systems employing SMF-DCF with RZ-pulse formats of the signals are more resilient to XPM and FWM impairments and SPM can be considered to be the major shortfalls in the system [5, 7, 12, 13]. Furthermore, XPM can be considered to be negligible in DWDM system due to : (i) highly dispersive system e.g SSMF-deployed systems; (ii) large channel spacing and (iii) high spectral efficiency. For transmission system operating at 40Gbps, using SSMF 17 ps/(nm.km) at 1550 nm and 0.8 nm spacing between 2 adjacent DWDM wavelengths, $L_w \approx 2.94\ km$. The XPM would be taken in to account for the systems deploying Non-zero dispersion shifted fibre (NZ-DSF) whose dispersion facto is very low. The development of the Simulator integrating these nonlinear impairments, the intra-channel nonlinear effects-XPM for DWDM systems will be reported in the near future. In this paper we assume that the transmission system is operating below the nonlinear limit. Indeed in Section IV the experimental demonstration of the optical systems shows this behavior. The other critical degradation factors to the DPSK/DQPSK system is the non-linear phase noise due to the fluctuation of the optical intensity caused by ASE noise via Gordon-Mollenauer effect. [14]. Receiver noise and electrical amplifier noise also taken into account.

3 MATLAB™ SIMULINK SIMULATOR

3.1 The DPSK transmitter model

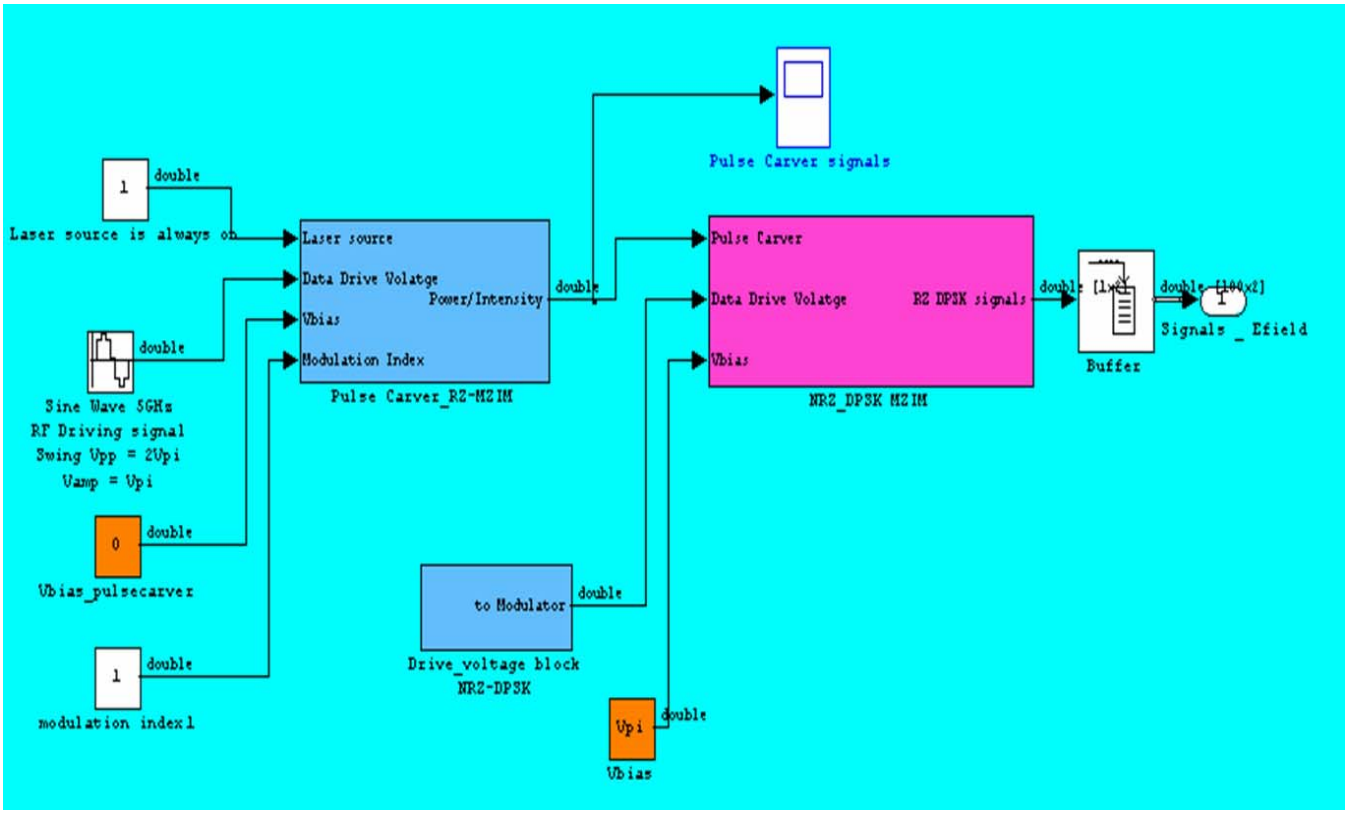

Fig. 4. Simulink model of DPSK transmitter (RZ or NRZ pulse formats)

There are two principal blocks of the photonic transmitter: the photonic pulse carver and the data modulator as described above. The lightwave source is presented as a pure sinusoidal signal generator. The linewidth of a laser source can be modeled by integrating a Lorentzian spectrum in the frequency domain and then taking an IFFT for generation of time domain lightwaves. The hidden structures of the pulse carver and data modulator are not described.

3.2 DPSK balanced receiver

Similarly a MZDI balanced receiver can be implemented in the Simulink platform as shown in Fig. 5. It is noted that the complex envelop of the optical field after the fibre propagation is converted into the magnitude and phase components. The phase part is the fed into the MZDI, hence the phase of the consecutive bits can be combined. Thus the MZDI can act as a phase comparator. Unlike in electronic

wireless receiver this phase comparison is performed after the detection process, photonic-opto-electronic balance receiver described here performs the photonic phase differential demodulation prior to the opto-electronic detection. This is the superiority of the photonic processing so that the ultra-wideband channel can be demodulated to overcome the electronic limitation.

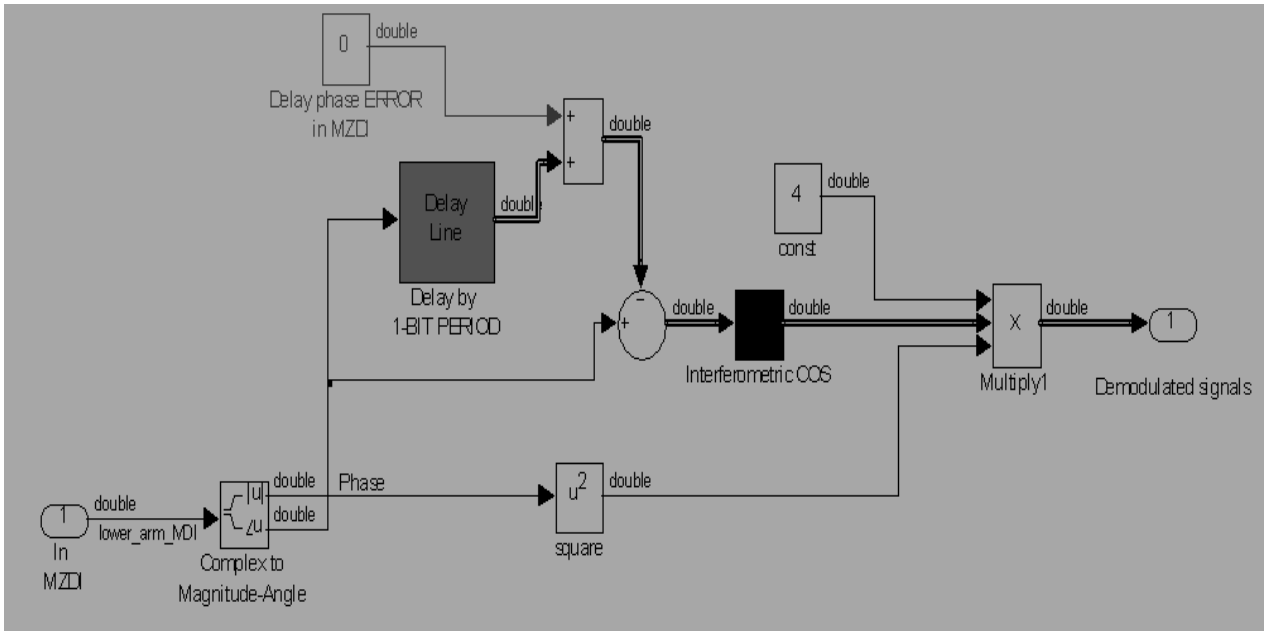

Fig. 5. Simulink model of DPSK balanced receiver

3.3 Optimized SSFM with SPM

The symmetrized SSFM can be optimized by: (i) split-step length that satisfies the constraint for the convergence; (ii) evaluation of incident peak power. If it is lower than the threshold of nonlinearities of the transmission fibre, the SPM effect can be neglected and SSFM will be switched to the Low Pass Transfer Function (LPTF) method that involves only the fibre dispersion and attenuation effects. The LPTF of the fibre is given as :

$$H_f(f) = \exp\left\{-j\left[(1/2)\beta_2^{'}\varpi^2 + (1/6)\beta_3^{'}\varpi^3\right]L\right. \tag{5}$$

where $\varpi = 2\pi f$, L is length of transmission and

$$\beta_2^{'} \cong -\frac{\lambda^2}{2\pi c}D \tag{6}$$

$$\beta_3^{'} \cong \left(\frac{\lambda}{2\pi c}\right)^2 \left(2\lambda D + D'\lambda^2\right) \tag{7}$$

with D is the fibre chromatic dispersion parameter at λ.

3.4 Optimized SSFM with SPM and XPM

XPM-induced degradation on DWDM system performance is not a strong function of number of channels [15]. Therefore, 3-channel modeling system can be sufficient for system investigation on the effects of XPM. The integration XPM into SSFM follows the following scheme [16]:

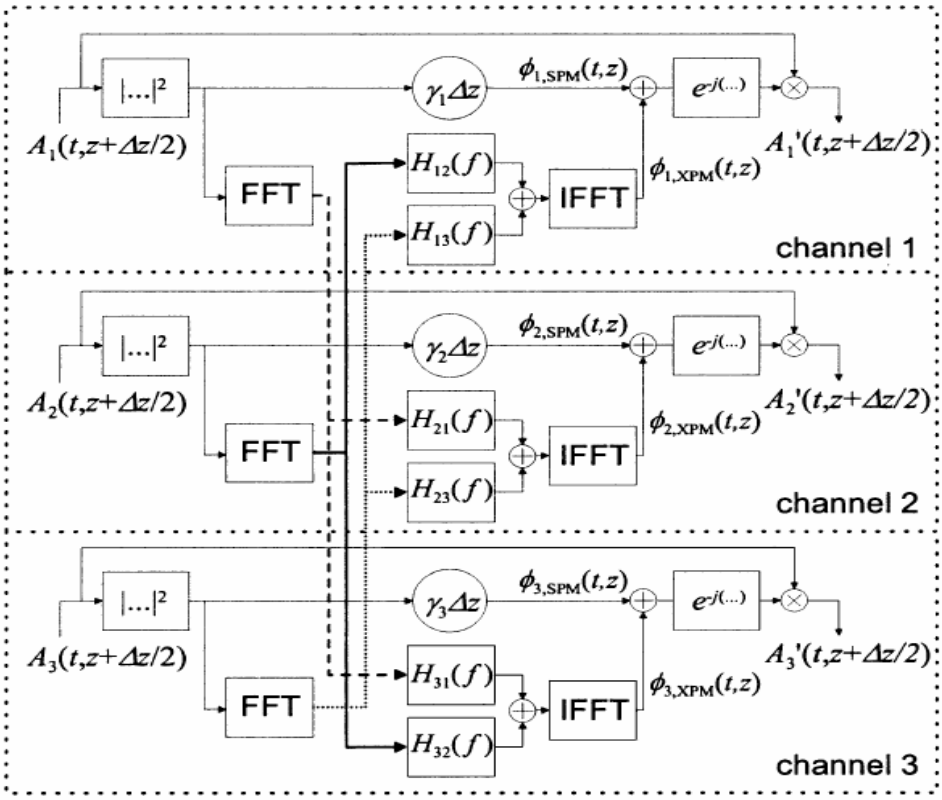

Fig. 6. Schemes for integration of XPM effects

$$H_{ik}(f) = 4\gamma_i \frac{\sin\left[\left(\alpha - j2\pi f d_{ik}\right)\Delta z/2\right]}{j\left(\alpha - j2\pi f d_{ik}\right)} \tag{8}$$

$$d_{ik} \equiv L_W = \frac{T_0}{\left|v_g^{-1}(\lambda_i) - v_g^{-1}(\lambda_k)\right|} \approx \frac{T_0}{D\Delta\lambda} \tag{9}$$

with T_0 is the bit period and $v_g(\lambda_i)$ is the group velocity of λ_i. The XPM effect can be integrated into the propagation model with ease. Similar to the determination of the linear-nonlinear region of the propagation model, the SSFM has been optimized by the checking the propagation position (z) compared to the walk-off length. The walk-off length is the main constraint for nonlinear interaction between two or multiple pulses when the XPM effects occur. More specifically, XPM can be considered to have no effects when the faster moving pulse completely walks through the slower moving pulses [17]. Furthermore, the XPM effects have been reported to be mainly significant in the first walk-off length [18]. If L_W is exceeded, XPM ceases and SSFM can be switched back to (4).

3.5 Polarization Mode Dispersion (PMD)

The PMD effect can be implemented in the model by two ways: (i) statistical noise complying Maxwellian distribution as follows [19]:

$$f(\Delta\tau,\Delta z)=\frac{2(\Delta\tau)^2}{\sqrt{2\pi}q^3}\exp\left\{-\frac{(\Delta\tau)^2}{2q^2}\right\}\quad \Delta\tau\geq 0 \tag{10}$$

where $\Delta\tau$ is differential group delay and q is a function of Δz - transmission span length. The expression of q is:

$$q=\sqrt{\frac{q}{8}}\delta_\tau\sqrt{\Delta z} \tag{11}$$

δ_τ is commonly termed as the "fibre PMD" and normally in the range of $0.1\text{-}0.2\ \text{ps}/\sqrt{\text{km}}$

(ii) The second method which is commonly implemented is that the fibre propagation is split into two distinct paths representing two states of polarizations (PSP). The fibre transfer function for first-order PMD is given by [20]

$$H_f(f)=H_{f+}(f)+H_{f-}(f) \tag{12}$$

$$\text{where}\quad H_{f+}(f)=\sqrt{\gamma}\exp\left[j2\pi f\left(-\frac{\Delta\tau}{2}\right)\right]\ \text{and}\ H_{f-}(f)=\sqrt{\gamma}\exp\left[j2\pi f\left(-\frac{\Delta\tau}{2}\right)\right] \tag{13}$$

4 SIMULATION RESULTS

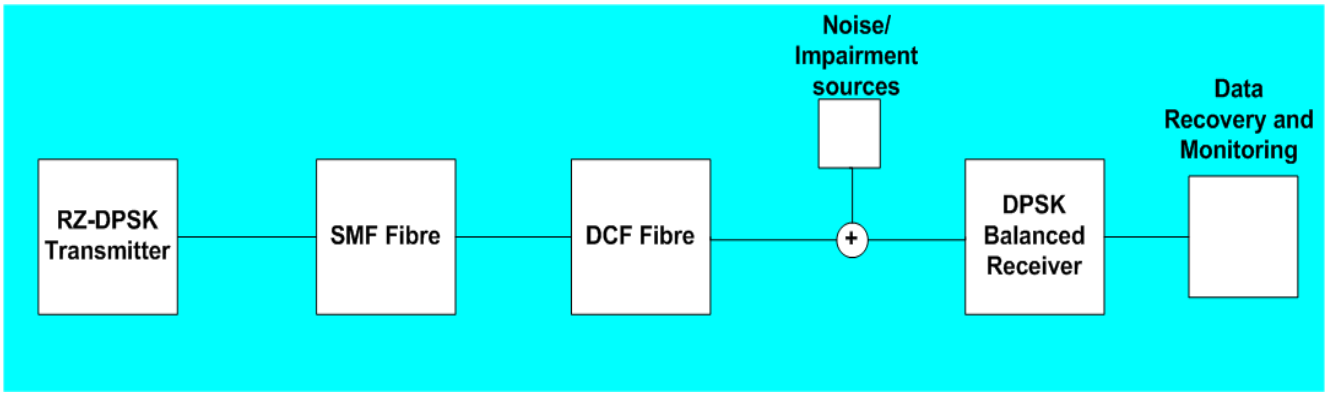

Fig. 7. Simulink model of the transmission test system.

A 10 km SSMF anomalous dispersion transmission length and a 85% dispersion compensation fibre section are integrated into the simulation model as shown in Fig. 7. The eye diagrams of the a PRBS DPSK encoded signals at the out put of the transmitters and at the output of the MZDI ban\lanced receiver are shown in Figs. 9 and 8 respectively.

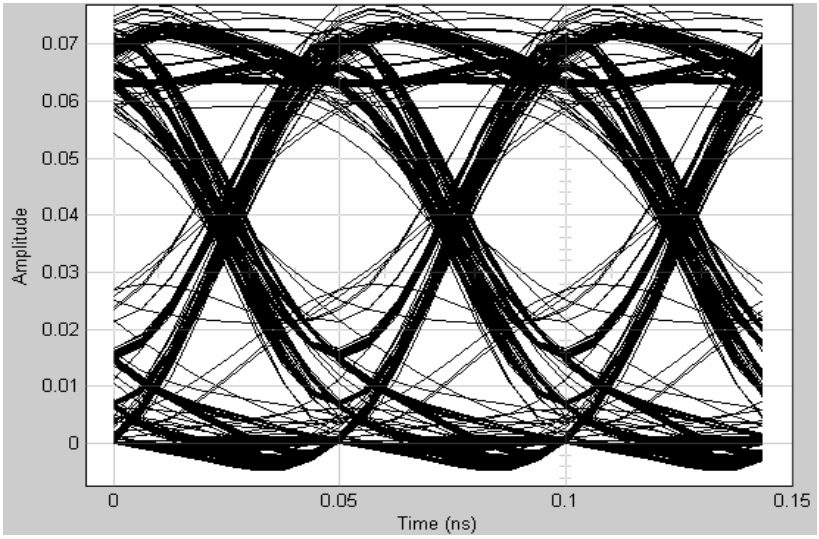

Fig. 8. A typical simulated eye diagram at the output of the MZDI balanced receiver for 50ps pulses. – 20 Gb/s

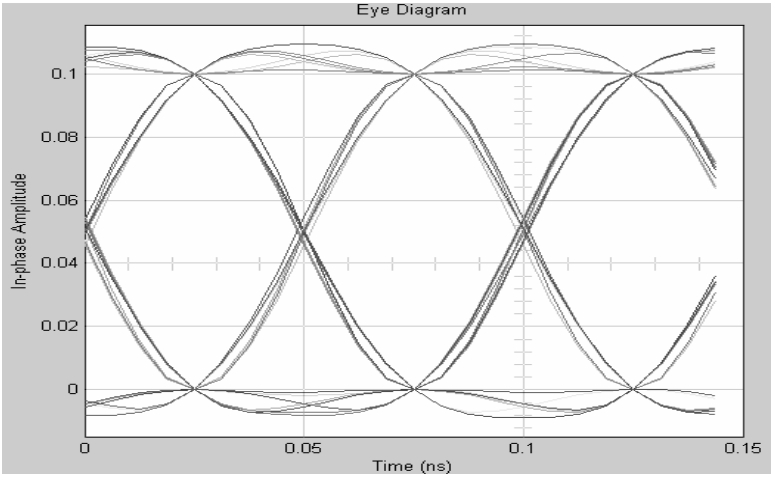

Fig. 9. Simulated eye diagram at the out put of the DPSK transmitter

5 EXPERIMENTAL DEMONSTRATION

The experiment set up for investigation of the dispersion tolerance of various modulation formats is shown in Fig. 9 inlcuding the transmitter, the receiver and necessary optical components and transmission and compensation fibres.

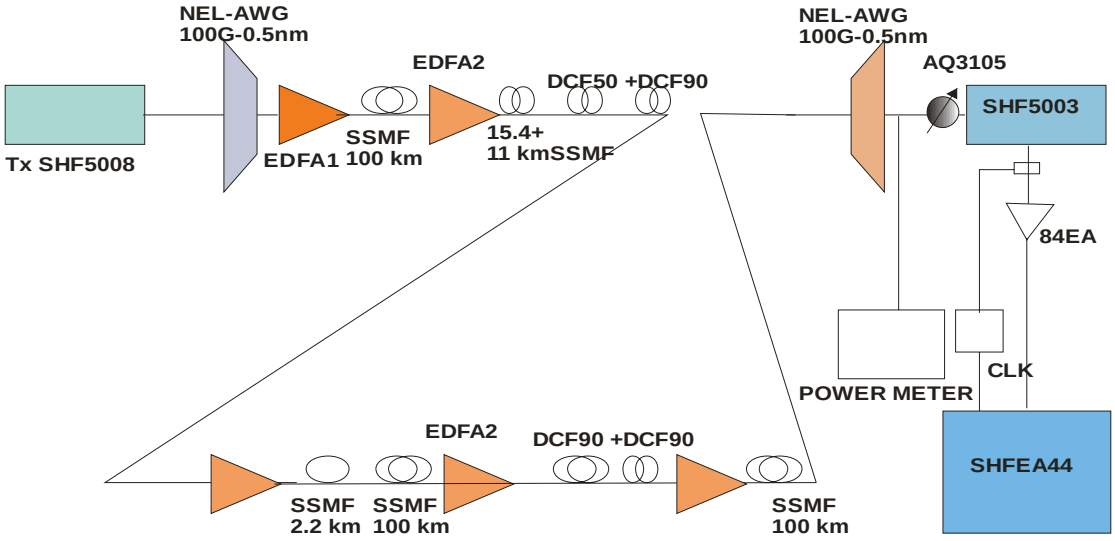

Fig. 10. Setup of the 40Gb/s experiment for investigation on dispersion tolerance of various ASK and DPSK modulation formats over 3220 SSMF and 328km effective dispersion compensation

Laser source centre wavelength: 1551.72 nm; pulse pattern of PRBS is 2^{31} -1. Equipment used in the experiment are: (i) 40Gb/s Tx is SHF 5003 DPSK Transmitter which can generate both ASK and DPSK data; (ii) In case of ASK, "Lab Buddy" Optical Receiver (45 GHz with built-in amplifier) is used; (iii) In case of DPSK, SHF 5008 DPSK receiver is used. Also, the Electrical Amp is utilized for signal conditioning the EA; (iv) JDS 1.2 nm filter was utilized after EDFA to decrease the ASE noise level; (v) Power launched into SMF (right after the Tx) is below the nonlinear SPM effects. (about 4 dBm),. However the launched power is very conservative and tabulated below:

Modulation/ formats	NRZ-ASK	RZ-ASK	CSRZ-ASK	NRZ-DPSK	RZ-DPSK	CSRZ-DPSK
Launched Power (dBm)	-4.2	-7.7	-6.2	-3.1	-6.2	-4.8

The optical spectra measured at the output of the transmitter for different modulation formats at 40Gb/s bit rate are shown in Fig. 10 and Fig. 11 for phase and amplitude modulation with RZ, NRZ and CSRZ formats respectively.

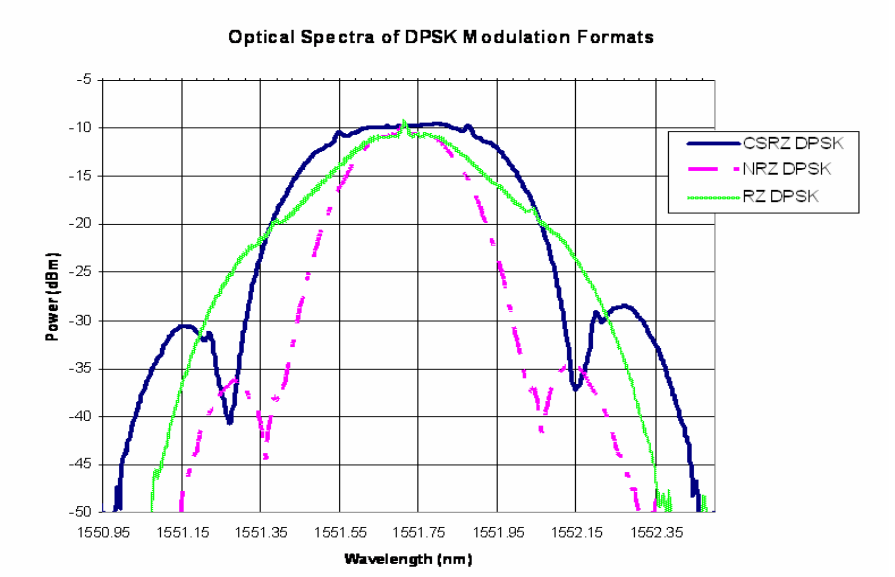

Fig. 11. Optical spectra of modulation formats CS-RZ, NRZ DPSK and RZ DPSK. Note the total signal energy levels of different modulation formats.

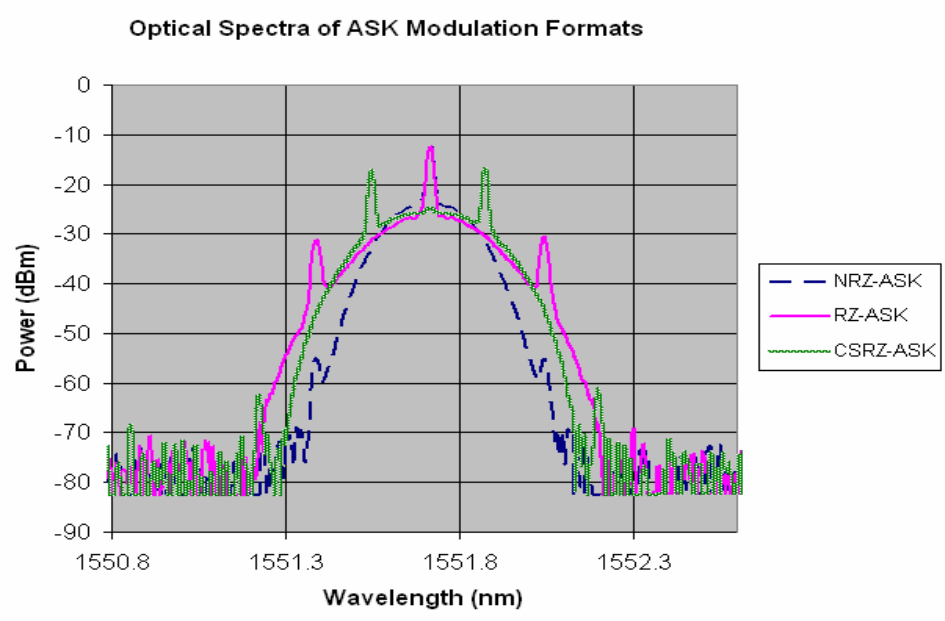

Fig. 12. Optical spectra of ASK modulation formats of NRZ, RZ and CSRZ.

We measure the dispersion tolerance of the transmitter and MZDI balanced receiver set for DPSK modulation with RZ, NRZ and CSRZ formats under the transmission length of 1 to 4 km and over 320 km standard SMF compensated by a dispersion compensating module of an 328 km SSMF dispersion compensation factor. The receiver sensitivities of the systems are shown and noted in Fig. 12(a) and (b) for 3km (non-compensating) and 320km SSMF (with compensation) transmission respectively. A 5dB improvement over the RZ-DPSK is achieved if CS-RZ format is used for DPSK modulation.

Fig. 13 and Fig.14 illustrate the eye diagrams of 40 Gb/s transmission for evaluation of dispersion tolerance with the transmission fibre SSMF of length 0-4 km (top to bottom) for ASK and DPSK modulation methods of different formats respectively. Note the eye diagrams of DPSK modulation formats and optimum sampling threshold are required for these formats.

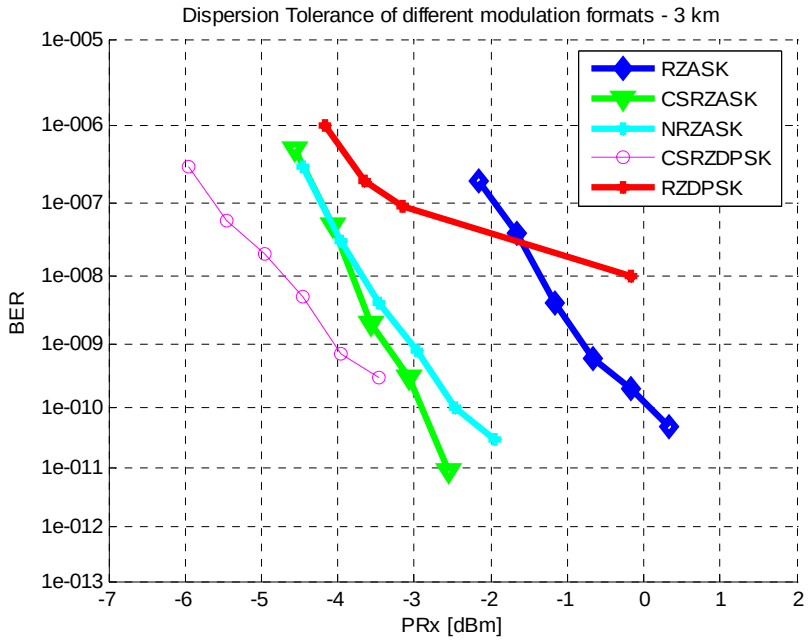

(a)

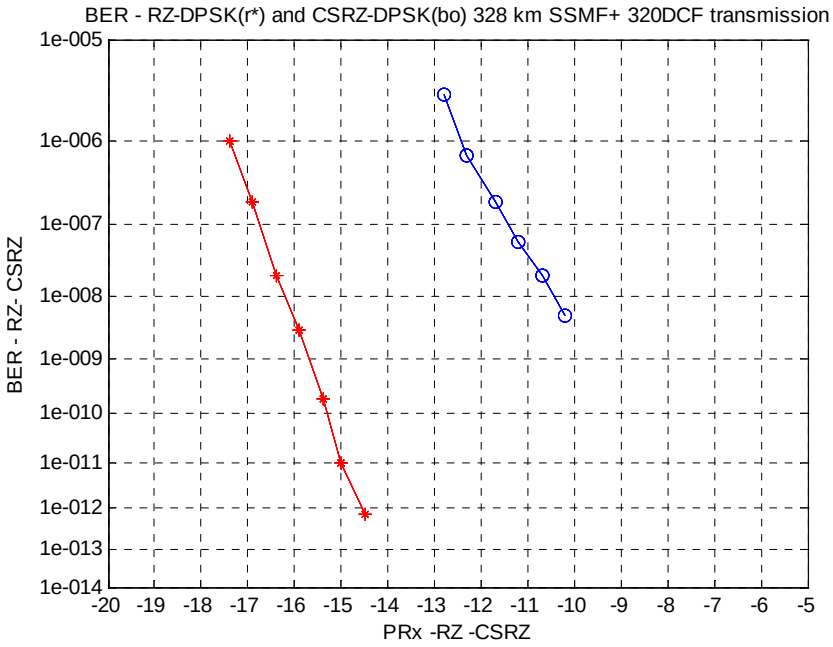

(b)

Fig. 13. Experimental BER of different modulation formats versus receiver sensitivity (a) 3 km SSMF (b) 328 kmSSMF + compensating fibres. Note: MUX is NEL AWG 0.5 nm 100 GHz Spacing and DEMUX is 1.2 nm OF (thin film structure) (see red curve) – blue is for NEL-AWG+NEL-AWG (100 GHz spacing and 0.5 nm BW) as MUX and DEMUX

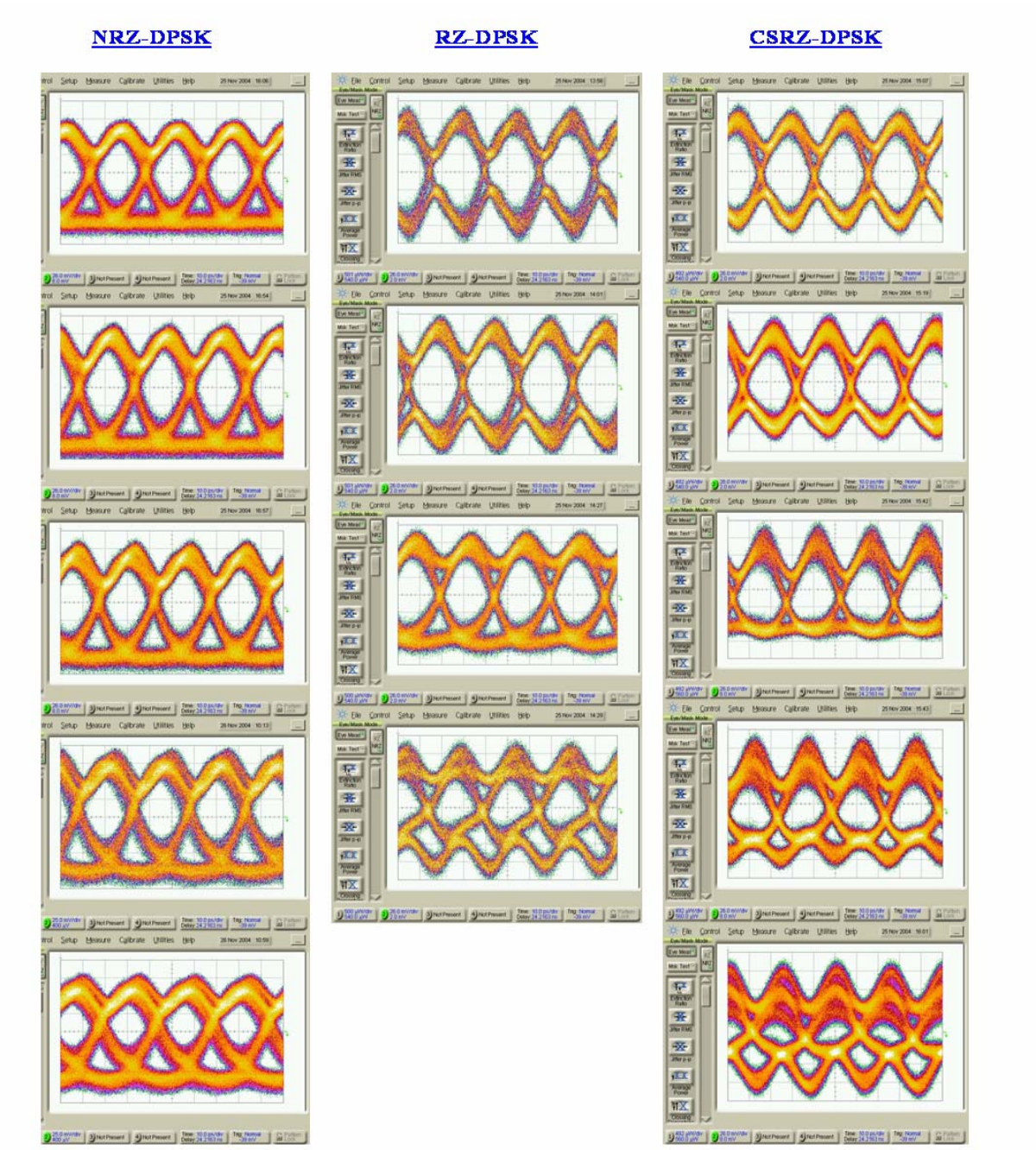

Fig. 14 Received eye diagrams of 40Gb/s differential phase modulation formats over 0-4 Km SSMF (top to bottom). Note: the plug-in of the sampling oscilloscope is a 50G bandwidth Agilent type.

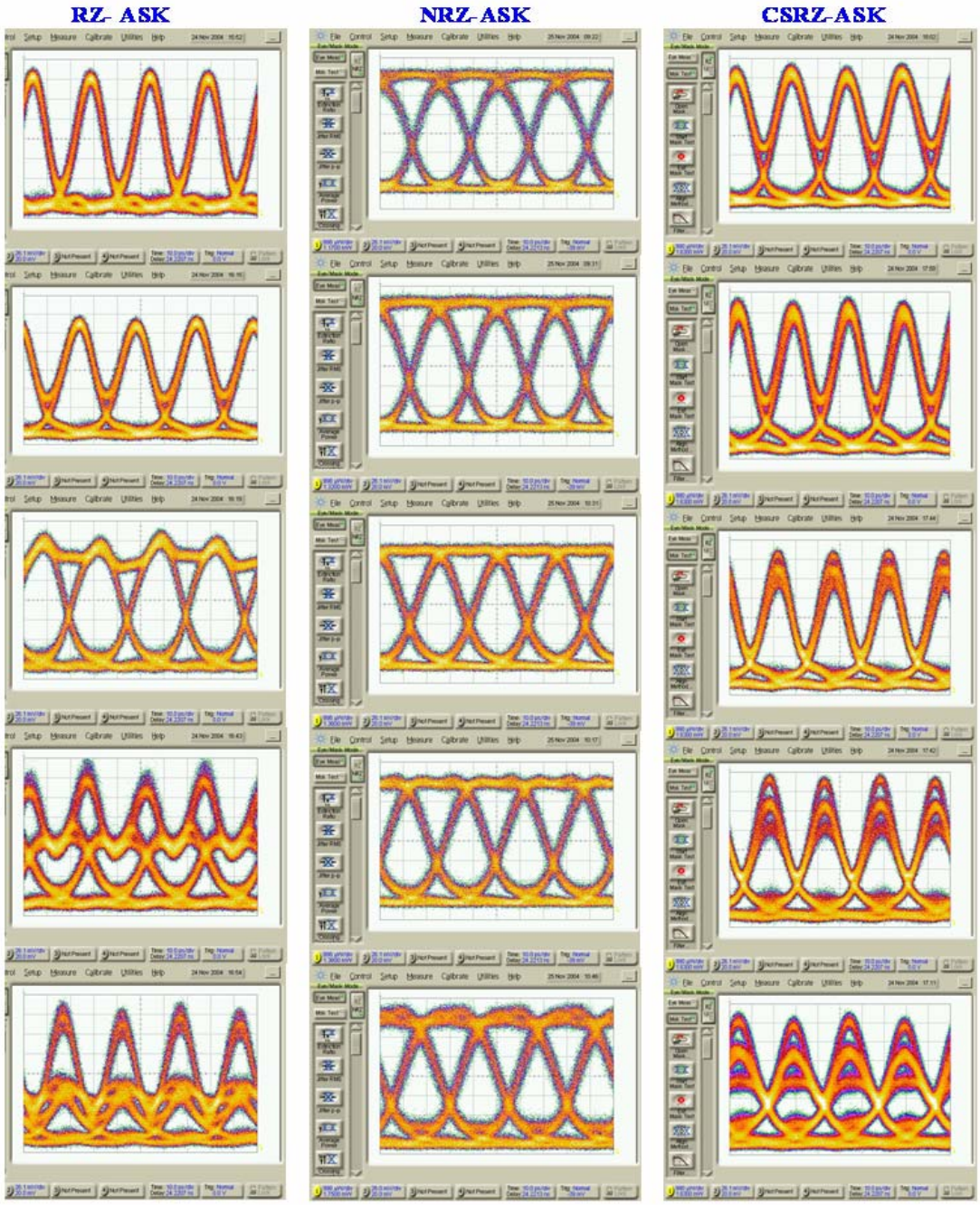

Fig. 15. Received eye diagrams of 40 Gb/s different ASK modulation formats over 0-4 km SMSMF (top to bottom)

6 CONCLUDING REMARKS

We have demonstrated the experimental and Simulink modeling of amplitude and phase modulation formats at 40 Gb/s optical fibre transmission. A novel modified fibre propagation algorithm has been used to minimize the simulation processing time and optimize its accuracy. The principles of amplitude and phase modulation, encoding and photonic-opto-electronic balanced detection and receiving modules have been demonstrated via Simulink modules and corroborated with experimental receiver sensitivities. The XPM and other fibre nonlinearity such as the Raman scattering, four wave mixing will be integrated in our Simulink model. Other modulations formats such as multi-level M-DPSK, M-ASK that offer narrower effective bandwidth, simple optical receiver structures and no chirping effects would also be integrated. These systems will be reported in future works. The effects of the optical filtering components in DWDM transmission systems to demonstrate the effectiveness of the DPSK and DQPSK formats, have been measured and will be reported in future publications. Finally, further development stages of the simulator together with simulation results will be reported in future works.

ACKNOWLEDGMENT

The authors acknowledge several fruitful discussions and advices from Dr. K. Clarke, Dr. G. Dhosi and Dr. F. Ruhl of Tesltra Corporation (Research Laboratories) of Clayton Victoria Australia and Dr. W.S. Lee of SHF Communications Technology AG of Berlin Germany for advices and friendships. We also thank Telstra Corporation for the set up of the transmission systems. The loan of the SHF-5003 and HF-5008 Transmitter and Receiver from SHF Communications Technology AG is greatly appreciated.

REFERENCES

[1] W. A. Atia and R. S. Bondurant, "Demonstration of return-to-zero signaling in both OOK and DPSK formats to improve receiver sensitivity in an optically preamplified receiver," presented at Lasers and Electro-Optics Society 1999 12th Annual Meeting. LEOS '99. IEEE, 1999.

[2] A. H. Gnauck, & Winzer .P.J., "Phase-Shift-Keyed Transmission," *OFC 2004*, vol. TuF5, 2004.

[3] H. Kim and A. H. Gnauck, "Experimental investigation of the performance limitation of DPSK systems due to nonlinear phase noise," *Photonics Technology Letters, IEEE*, vol. 15, pp. 320-322, 2003.

[4] P. J. Winzer, S. Chandrasekhar, and H. Kim, "Impact of filtering on RZ-DPSK reception," *Photonics Technology Letters, IEEE*, vol. 15, pp. 840-842, 2003.

[5] H. Kim, "Differential phase shift keying for 10-Gb/s and 40-Gb/s systems," presented at Advanced Modulation Formats, 2004 IEEE/LEOS Workshop on, 2004.

[6] S. Bhandare, D. Sandel, A. F. Abas, B. Milivojevic, A. Hidayat, R. Noe, M. Guy, and M. Lapointe, "2/spl times/40 Gbit/s RZ-DQPSK transmission with tunable chromatic dispersion compensation in 263 km fibre link," *Electronics Letters*, vol. 40, pp. 821-822, 2004.

[7] T. Mizuochi, K. Ishida, T. Kobayashi, J. Abe, K. Kinjo, K. Motoshima, and K. Kasahara, "A comparative study of DPSK and OOK WDM transmission over transoceanic distances and their performance degradations due to nonlinear phase noise," *Lightwave Technology, Journal of*, vol. 21, pp. 1933-1943, 2003.

[8] C. Xu, X. Liu, L. F. Mollenauer, and X. Wei, "Comparison of return-to-zero differential phase-shift keying and ON-OFF keying in long-haul dispersion managed transmission," *Photonics Technology Letters, IEEE*, vol. 15, pp. 617-619, 2003.

[9] U.-V. Koc and X. Wei, "Combined effect of polarization-mode dispersion and chromatic dispersion on strongly filtered /spl pi//2-DPSK and conventional DPSK," *Photonics Technology Letters, IEEE*, vol. 16, pp. 1588-1590, 2004.

[10] E. Ip and J. M. Kahn, "Power Spectra of Return-to-Zero Optical Signals," *submitted to J. Lightwave Tech*, July, 2004.

[11] "Operating Manual, DPSK Optical Transmitter - SHF 5003," SHF Communication Technologies AG - Germany.

[12] Elbers et al, Int. J. Electron. Commun. (AEU) 55, pp 195-304, 2001.

[13] T. Tokle., C. Peucheret., and P. Jeppesen, "Advanced Modulation Fortmas in 40Gbit/s Optical Communiaction systems with 80 km Fibre Spans.," *Elsevier Science*, July 2003.

[14] J.P. Gordon. and L. F. Mollenauer, "Phase noise in photonic communications systems using linear amplifiers," *Opt. Lett.*, vol. 15, pp. 1351-1353, Dec. 1990.

[15] D. Marcuse, A. R. Chraplyvy, and R. W. Tkach, "Dependence of cross-phase modulation on channel number in fiber WDM systems," *Lightwave Technology, Journal of*, vol. 12, pp. 885-890, 1994.

[16] J. Leibrich and W. Rosenkranz, "Efficient numerical simulation of multichannel WDM transmission systems limited by XPM," *Photonics Technology Letters, IEEE*, vol. 15, pp. 395-397, 2003.

[17] G. P. Agrawal, *Nonlinear Fibre Optics*, 3rd ed. ed. California: Academic Press, 2001, pp.13.

[18] M. Shtaif and M. Eiselt, "Analysis of intensity interference caused by cross-phase modulation in dispersive optical fibers," *Photonics Technology Letters, IEEE*, vol. 10, pp. 979-981, 1998.

[19] A. Carena, V. Curri, R. Gaudino, P. Poggiolini, and S. Benedetto, "A time-domain optical transmission system simulation package accounting for nonlinear and polarization-related

effects in fiber," *Selected Areas in Communications, IEEE Journal on*, vol. 15, pp. 751-765, 1997.

[20] G. Jacobsen, "Performance of DPSK and CPFSK systems with significant post-detection filtering," *Lightwave Technology, Journal of*, vol. 11, pp. 1622-1631, 1993.